Piotr Lalewicz
mgr inż.
Politechnika Wrocławska
Wydział Budownictwa Lądowego i Wodnego
Katedra Dróg, Mostów, Kolei i Lotnisk
piotr.lalewicz@pwr.edu.pl

Danuta Bryja
dr hab. inż., prof. uczelni
Politechnika Wrocławska
Wydział Budownictwa Lądowego i Wodnego
Katedra Dróg, Mostów, Kolei i Lotnisk
danuta.bryja@pwr.edu.pl

DOI: 10.35117/A_ENG_21_06_07_03

Visco-elastic contact spring in numerical simulations of train – track system vibrations

Abstract: In train – track coupled systems, interaction between subsystems occurs in wheel-rail contact. The most common contact model is perfectly elastic, linearized Hert'z spring. It has wide range of application in numerical simulations. In more detailed interaction models, the energy dissipation in wheel-rail contact is taken into account. There are no known comparisons of these models in the literature, that would indicate the effects of a specific solution application.
In this paper, the main purpose is to analyze and compare the effects of two contact models in terms of numerical simulations of train – track vibrations. The reference contact model taken into account is linearized, perfectly elastic Hert'z spring. The second spring, proposed by the authors is enriched with viscous element based on hysteresis damping. Application of both models, and its effects were examined in plane, train – track vibrations simulations with threshold inequality excitation in the middle of the track length. Concluding from the analyzes performed, it was found that viscoelastic contact model application is important, when track stresses and fatigue are being investigated. In addition, it was found that neglecting the damping element in contact model reduces the probability of the wheel – rail contact loss phenomenon, and thus leads to incorrect identification of its occurrence.

Keywords: Wheel/rail contact; Hertz contact; Linearized contact spring; Train/track dynamics

Introduction

In numerical modeling of coupled systems, where we deal with the mutual interaction of bodies, the key element is the model of the contact of these bodies through which the interaction takes place. The selection of an appropriate numerical model of the contact zone allows for a correct description of the phenomena occurring between the bodies.

In a coupled train-track system, the contact between subsystems occurs at the contact of each wheel with the rail and is rolling. The method of modeling this contact depends significantly on the assumed goal of numerical simulations, and this depends on the type of analyzed issues. They can be broadly divided into two groups - issues focused on the analysis of the problems of the mechanics of a railway vehicle, and issues focused on the analysis of the railway track. In the case of the first group of issues, contemporary spatial contact models are used, often very complex, built with the use of FEM (Bosso et al. [1]). These types of contact zone models are currently not used for the second group of issues, especially when

simulations are performed for the purposes of dynamic analyzes. The reason for excluding these models is the simulation time, which would exceed the computational possibilities available today.

Simplified contact models are usually used in simulations of track vibration caused by train runs. The simplest of them is the rigid contact, in which it is assumed that the displacements of the wheel and rail are the same, which is a great simplification because then the deformability of the contacting surfaces is completely ignored. The rigid contact model is so far used in simulations of vibrations of bridge-track-train systems (e.g. Xu and Zhai [14]). However, the most popular contact model currently used, among others, by Zhai [16, 17, 18], Klasztorny and Podwórna [9], Yongle Li [15] and described, for example, in Esveld's monograph [3], is the so-called Hertz's bond, i.e. a model in the form of an elastic bond with the characteristics determined on the basis of Hertz's contact theory. In richer variants of the Hertz contact model, the dissipation of energy at the contact point of the wheel with the rail is additionally taken into account. An example is a model proposed by Pombo et al. [10], in which energy dissipation is described by introducing a damper representing hysteresis suppression according to the Lankarani and Nikravesh model [7]. The listed basic variants of contact models are used alternatively in the methods of track vibration simulation, however, the literature lacks comparisons of these models indicating the effects of applying a specific solution.

The main goal of this work is a comparative analysis of two selected contact bonds, and this analysis was preceded by our own formulation of the elastic-damping contact bond, in which the elastic element is a linearized Hertz elastic bond and the damping element corresponds to the hysteresis damping. Therefore, in numerical simulations, the linearized Hertz-type elastic constraint was considered in two variants - without damping and with hysteresis damping. The effects of applying these bonds were investigated on the basis of a comparison of the simulation results of vertical track vibrations with the threshold unevenness through which a train, which constitutes a set of railway vehicles, passes. Each vehicle is modeled by a discrete dynamic system with ten degrees of freedom composed of masses representing the body, two two-axle bogies, and wheel sets. The masses are connected by systems of viscoelastic bonds that model the two-stage suspension of the vehicle. Based on the performed numerical analyzes, a thesis was made that the use of the wheel-rail contact model enriched with hysteresis suppression makes sense when the tests are focused on the track strain and fatigue effects in the track and railway vehicle. Moreover, it was found that omitting the damping in the contact zone slightly reduces the probability of the loss of contact, and therefore does not lead to the correct identification of this phenomenon.

Contact springs

The Hertz elastic bond, which is a classic model of contact between the wheel and rail, has been briefly described, for example, in the Esveld monograph [3]. In this model, both the rail and the wheel are treated as non-deformable bodies, and an elastic band is introduced between these bodies, which describes in a simplified manner the deformation of the bodies at the point of contact (crush). The stiffness of the bond k_{H} is determined using Hertz's theory.

According to Hertz's theory describing the contact of two deformable bi-curvature bodies, the collapse of the bodies δ at their point of contact, due to the contact force F_{H} acting between these bodies is written by the formula (cf. Johnson [4])

$$\delta = \left(\frac{9F_{\mathrm{H}}^{\ 2}}{16E^{*2}R_e} \right)^{1/3} F_2(e) \tag{1}$$

where $E^*$and R_e are constants depending on the material parameters and the curvature of the bodies, respectively. These constants are defined by formulas

$$\frac{1}{E^*}=\frac{1-\nu_1^{\,2}}{E_1}+\frac{1-\nu_2^{\,2}}{E_2},\qquad R_e=\frac{1}{2}\frac{1}{\sqrt{\frac{1}{4}\left(\frac{1}{R_{1,y}R_{1,x}}+\frac{1}{R_{2,y}R_{2,x}}\right)}} \tag{2}$$

$F_2(e)$ is a correction factor depending on the curvature of the contacting bodies, which in engineering problems with circular curvatures can be assumed to be equal to one ([4]). Transforming (1) taking into account that $F_2(e)$ =1, and assuming that the contacting bodies are made of steel with similar material parameters, a non-linear relationship between the contact force and the working force of the material at the point of contact is obtained

$$F_{\mathrm{H}}=C_{\mathrm{H}}\delta^{\frac{3}{2}} \tag{3}$$

where

$$C_{\mathrm{H}}=\frac{4G\sqrt{R_e}}{3(1-\nu)}=\frac{2E\sqrt{R_e}}{3(1-\nu^2)} \tag{4}$$

The constant C_{H}, called the Hertz constant, is expressed by the parameter R_e and the material constants: elastic modulus E or transverse G and Poisson's ratio ν.

The non-linear relationship (3) is quoted in various contemporary publications on the wheel-rail contact, e.g. in [6, 13], where it is the basis for deriving the formula for the so-called Hertz's equivalent stiffness, which determines the linearized relation between the dynamic contact force and material compaction

$$F_{\mathrm{H}}=k_{\mathrm{H}}\delta \tag{5}$$

The equivalent stiffness k_{H} is a characteristic of the linear-elastic Hertz contact bond, which is commonly used in problems of simulating vibrations of train-track systems. Strictly speaking, the Hertz stiffness is a derivative of the contact force (3), which is

$$\frac{dF_{\mathrm{H}}}{d\delta}=\frac{3}{2}C_{\mathrm{H}}\delta^{\frac{1}{2}} \tag{6}$$

After considering that

$$\delta^{\frac{1}{2}}=C_{\mathrm{H}}^{\;-\frac{1}{3}}F_{\mathrm{H}}^{\;\frac{1}{3}} \tag{7}$$

which results directly from equation (3), we get

$$\frac{dF_{\mathrm{H}}}{d\delta}=\frac{3}{2}C_{\mathrm{H}}^{\;\frac{2}{3}}F_{\mathrm{H}}^{\;\frac{1}{3}} \tag{8}$$

The basis for linearization of the relation (3) to the form (5) is to accept the simplification that the derivative (8) is constant, i.e. it does not depend on changes in the contact force F_{H} over time, and its value can be calculated on the basis of the static wheel pressure force on the Q_{H} rail around which the dynamic contact force F_{H} oscillates. The result of this simplification is

$$k_{\mathrm{H}}=\frac{3}{2}C_{\mathrm{H}}^{\;\frac{2}{3}}Q_{\mathrm{H}}^{\frac{1}{3}}=\frac{3}{2}\sqrt[3]{\frac{4Q_{\mathrm{H}}E^2\sqrt{R_{\mathrm{rail}}R_{\mathrm{wheel}}}}{9(1-\nu^2)^2}}=\sqrt[3]{\frac{3Q_{\mathrm{H}}E^2\sqrt{R_{\mathrm{rail}}R_{\mathrm{wheel}}}}{2(1-\nu^2)^2}} \tag{9}$$

given, among others by Esveld [3]. The Hertz constant C_{H} in formula (9) was calculated on the basis of (4) assuming that the radius of curvature of the rail in the longitudinal direction is infinitely large and that the wear of the wheel leads to a flattening of its transverse profile, which leads to the contact of two cylindrical surfaces with radii of curvatures R_{szyny} and R_{kola}, therefore $R_e=\sqrt{R_{\mathrm{szyny}}R_{\mathrm{kola}}}$.

In order to determine the applicability of the approximate relation (5), Figure **1** shows exemplary graphs of the relationship between the contact force F_{H} and the material crush δ,

Hertz's equivalent stiffness (9) was calculated assuming two values of static pressure: Q_H = 138,5 kN as for the Shinkansen passenger train (dark gray line) and Q_H = 250 kN as for the freight train (light gray line). It can be observed that beyond the conventional limit of δ = 0,3 mm, the value of the contact force F_H determined from the nonlinear dependence (3) significantly differs from substitute solutions (5), therefore the linearized solutions are burdened with too much error. It can be assumed that they are acceptable below the limit δ = 0,3 mm, which corresponds to a contact force of about 400 kN or more. It should be noted that the range from 0 to 400 kN fully covers the values of the forces occurring at the wheel-rail interface in railway problems.

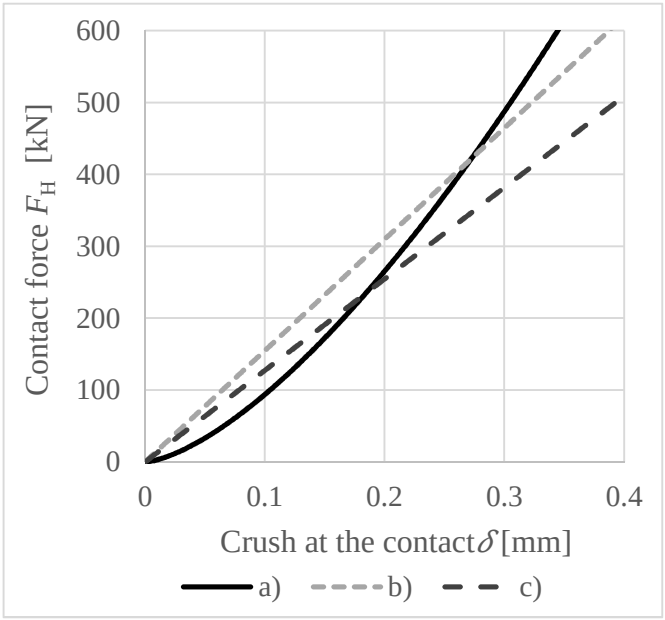

1. Contact force - crush relation:
a) nonlinear - formula (3), b) linearized – formula (5), freight car,
c) linearized - formula (5), passenger vehicle

The perfectly elastic contact models introduce some additional simplification. They assume that the process of deformation of the body is fully reversible, while in fact energy is lost due to, among other things, micro friction between molecules in the material's crystalline structure, the generation of heat and noise. The hysteresis phenomenon is used to describe the history of multiple loading and unloading of a material. It should be noted here that pure-elastic contact bond models constitute only a small group among the models used, for example, in MBS (Multi-Body Systems) problems. Skrinjar et al. [12] found that over 20 models of contact bond can be distinguished, most of which are elastic-damping bonds, in which the damping is described by the hysteresis damping coefficient χ. Nevertheless, a damped contact model is rarely used in train-to-track vibration simulations. One of the few examples is described in Shaban et al. [11], where the authors proposed the introduction of an elastic-damping bond at the wheel-rail interface based on the Lee and Wang model [8], in which the contact force is represented by the formula

$$F_H = C_H \delta^{\frac{3}{2}} + D_H \dot{\delta} \tag{11}$$

where

$$D_H = \chi \delta^{\frac{3}{2}} = \frac{3(1-e)}{4} \frac{C_H}{\dot{\delta}_0} \delta^{\frac{3}{2}} \tag{12}$$

wherein $\dot{\delta}_0$ is the initial speed of indenting the wheel into the rail, while e is the restitution coefficient, which for low speeds below 1 m / s is not subject to significant variability - for steel, a constant value can be assumed e = 0,93.

A similar elastic-damping contact bond was used by Pombo et al. [10]. To describe the relation, they used the model proposed by Lankarani and Nikravesh [7], which differs from the Lee and Wang model in a slightly different formulation of the hysteresis damping coefficient - the restitution coefficient is squared in it, therefore

$$D_{\mathrm{H}} = \chi\delta^{\frac{3}{2}} = \frac{3(1-e^2)}{4}\frac{C_{\mathrm{H}}}{\dot{\delta}_0}\delta^{\frac{3}{2}} \tag{13}$$

and the contact force is still expressed by the formula (11). This means that in both the Lee and Wang model [13] and the Lankarani and Nikravesh model [7] the damping bond is associated with an elastic bond with a nonlinear characteristic (3).

In this study, a simplified elastic-damping contact bond was proposed, in which the elastic element corresponds to the linearized Hertz elastic bond (5). It was assumed that in this case the contact force can be written as the following relation

$$F_{\mathrm{H}} = k_{\mathrm{H}}\delta + \chi\delta\dot{\delta} = k_{\mathrm{H}}\delta + \frac{3(1-e^2)}{4}\frac{k_{\mathrm{H}}}{\dot{\delta}_0}\delta\dot{\delta} \tag{14}$$

by analogy to (11) and (13). The second component of the relation (14) introduces a non-linear effect due to the presence of the coefficient $\delta\dot{\delta}$. In order to simplify the problem, the assumption used earlier to linearize the relationship (3) was consistently applied, and the formula component (14) related to the damping element of the contact bond was similarly linearized, relating it to the maximum static value δ_0, as the initial value around which the dynamic deformation of the bond oscillates δ. This simplification leads to a linear relation

$$F_{\mathrm{H}} = k_{\mathrm{H}}\delta + d_{\mathrm{H}}\dot{\delta} \quad \text{gdzie} \quad d_{\mathrm{H}} = \frac{3(1-e^2)}{4}\frac{k_{\mathrm{H}}}{\dot{\delta}_0}\delta_0 \tag{15}$$

which describes the simplified, elastic-damping contact bond mentioned in this work.

In order to apply the relation (15) in simulations of the coupled vibrations of the vehicle and the track, it is necessary to define the initial speed $\dot{\delta}_0$ denting the wheel into the rail. This problem is not unequivocally solved in the literature (Pombo et al. [10]), because the difficulty is that at any time t_i numerical simulation of the vibration process, the location of the contact changes as a result of the wheel rolling along the rail. It was assumed approximately that at any time t_i a new one-point contact between the wheel and rail is created, as well as new material compaction that builds up in local time τ from zero to the maximum static value δ_0, on which dynamic compaction is imposed $\delta(t_i)$ with speed $\dot{\delta}(t_i)$. It was assumed, that initial speed $\dot{\delta}_0$ wheel indentation into the rail is the speed at time τ achieving maximum static compaction δ_0. To determine this speed, the solution given in [7]

$$\dot{\delta}_0^2 = \frac{2(m_i + m_j)C_{\mathrm{H}}}{m_i m_j (n+1)}\delta_0^{\,n+1} \tag{16}$$

Derived on the basis of the equation describing the collision of two spherical bodies with masses m_i and m_j, which were formulated starting from the energy balance. Elastic strain energy was calculated as the work of the contact force resulting from Hertz's theory, which in the case of bodies made of steel is determined by the formula (3), and then n = 3/2. When introducing instead of (3) the linearized relation (5) should be substituted for (16) the equivalent stiffness k_{H} instead of Hertz's constant C_{H} and n = 1. Additionally, taking into

account that the weight of the rail with the ground is much greater than the weight of the wheel ($m_i >> m_j$) it is obtained approximately

$$\dot{\delta}_0^2 = \frac{2(m_i + m_j)k_{\mathrm{H}}}{m_i m_j (1+1)} \delta_0^{1+1} \approx \frac{k_{\mathrm{H}} \delta_0^{\,2}}{m_{\mathrm{wheel}}} \tag{17}$$

Taking into account on the basis of (15) that at the time τ to achieve the maximum static compaction there is a relation

$$Q_{\mathrm{H}} = k_{\mathrm{H}} \delta_0 + d_{\mathrm{H}} \dot{\delta}_0 \tag{18}$$

and

$$\frac{d_{\mathrm{H}}}{k_{\mathrm{H}}} = \frac{3(1-e^2)}{4} \frac{\delta_0}{\dot{\delta}_0} \tag{19}$$

it is obtained

$$\delta_0 = \frac{Q_{\mathrm{H}}}{k_{\mathrm{H}}} - \frac{d_{\mathrm{H}}}{k_{\mathrm{H}}} \dot{\delta}_0 = \frac{Q_{\mathrm{H}}}{k_{\mathrm{H}}} - \frac{3(1-e^2)}{4} \delta_0 \tag{20}$$

and hence

$$\delta_0 = \frac{4}{7-3e^2} \frac{Q_{\mathrm{H}}}{k_{\mathrm{H}}} \tag{21}$$

Assuming the restitution coefficient for steel is equal to e = 0,93, it can be roughly assumed that the initial (maximum static) compaction is $\delta_0 = 0,908 Q_{\mathrm{H}} / k_{\mathrm{H}}$.

Vibration simulation algorithm

Initial assumptions

To simulate the vertical vibrations of the track, the calculation algorithm described in [2] was used, based on the finite element method formulated in the Galerkin approach and referring to the plane computational model of the train-track system (Figure **2**). Appropriate modifications to the algorithm were introduced, allowing for an alternative consideration of Hertz-type contact springs - with and without suppression.

Due to the requirements of the method, it was assumed that the deformable section of the track has a finite length, and outside this section, the track is non-deformable. The deformable track section L is divided into two sections L_1 and L_2 significantly different in terms of the ground parameters, as a result of which a threshold unevenness appears at the junction of these sections.

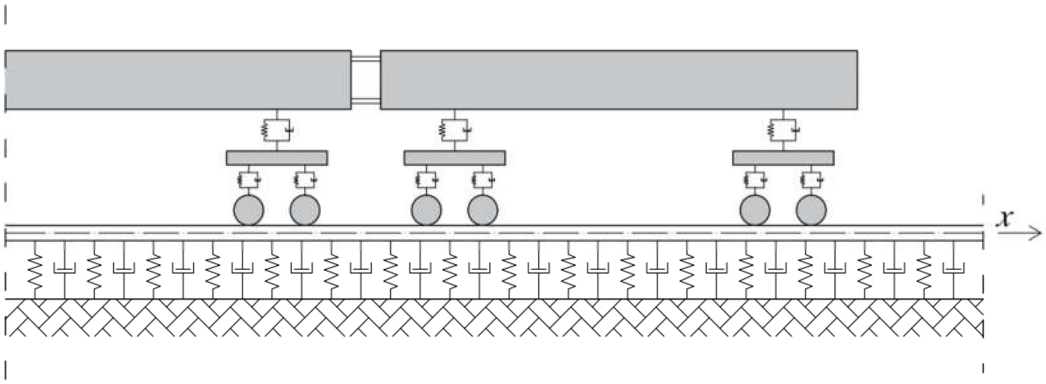

2. Diagram of the train-track system

In this model, the track is an Euler-Bernoulli beam resting on a Winkler springy foundation with damping, and railway vehicles are dynamic systems with ten degrees of freedom. The track is loaded with the forces of the wheelsets $R_j(t)$ varying in time, which are also the reactions of the contact bonds. The position of the wheelset number j at time t is described by the coordinate $s_j(t) = vt - d_j$, where v is the constant running speed of the train.

The interaction between two coupled dynamic subsystems: track and train is provided by contact bonds adopted alternatively as:

- two-sided, linearized Hertz-type springs, ideally elastic (as in [2]), then

$$R_j(t) = Q_j + k_{\mathrm{H}j}[V_j(t) - W_j(t)] \tag{22}$$

- two-sided, linearized Hertz-type springs, elastic-damping, where

$$R_j(t) = Q_j + k_{\mathrm{H}j}[V_j(t) - W_j(t)] + d_{\mathrm{H}j}[\dot{V}_j(t) - \dot{W}_j(t)] \tag{23}$$

where Q_j is here the static load of the j th wheel set, $V_j(t)$ is the vertical displacement of the wheelset, and $W_j(t)$ is the displacement of the track at the point of contact. The stiffness and the damping parameter of the contact bond result from the parallel connection of the two bonds introduced at the junction of each wheel of the set with the rail, hence, $k_{\mathrm{H}j} = 2k_{\mathrm{H}}$, $d_{\mathrm{H}j} = 2d_{\mathrm{H}}$ wherein formulas (9) and (15) it is necessary to substitute: $Q_{\mathrm{H}} = Q_j / 2$.

General form of the equations of motion for the train-track system

Vertical track vibration $w(x, t)$ are described by a differential equation of known form

$$EJ\frac{\partial^4 w(x,t)}{\partial x^4} + kw(x,t) + c\frac{\partial w(x,t)}{\partial t} + m\frac{\partial^2 w(x,t)}{\partial t^2} = \sum_{j=1}^{N} R_j(t)\delta(x - s_j) \tag{24}$$

This equation was transformed into a system of ordinary differential equations using the finite element method (in terms of Galerkin), which allows you to easily take into account different values of track substrate parameters (k and c) on sections L_1 and L_2. The system of equations written in matrix notation has the following general form

$$\mathbf{B}_{\mathrm{tt}}\ddot{\mathbf{q}}_{\mathrm{t}}(t) + \mathbf{C}_{\mathrm{tt}}\dot{\mathbf{q}}_{\mathrm{t}}(t) + \mathbf{K}_{\mathrm{tt}}\mathbf{q}_{\mathrm{t}}(t) = \tilde{\mathbf{F}}_{\mathrm{t}}(t) \tag{25}$$

A system of equations that describe the vibrations of the set of vehicles that make up the train

$$\mathbf{B}_{\mathrm{vv}}\ddot{\mathbf{q}}_{\mathrm{v}}(t) + \mathbf{C}_{\mathrm{vv}}\dot{\mathbf{q}}_{\mathrm{v}}(t) + \mathbf{K}_{\mathrm{vv}}\mathbf{q}_{\mathrm{v}}(t) = \tilde{\mathbf{F}}_{\mathrm{v}}(t) \tag{26}$$

The methodology typical for discrete systems was derived, i.e. based on the energy balance and Lagrange's equations. In order to facilitate the mathematical notation of the coupling of equations (25) and (26), the equations forming the system (25) have been arranged in such a way that the vector of displacements corresponding to the degrees of freedom of vehicles is divided into two blocks: $\mathbf{q}_{\mathrm{v}} = \mathrm{col}(\mathbf{r}, \mathbf{V}_{\mathrm{c}})$. The symbol "col" in this notation means a column matrix, the vector $\mathbf{r}$ corresponds to the internal degrees of freedom of the vehicles, and the vector $\mathbf{V}_{\mathrm{c}} = [V_1, V_2, ..., V_N]^{\mathrm{T}}$ it includes vertical displacements of successive wheel sets. Adequately to the block division of the vector $\mathbf{q}_{\mathrm{v}}$ all matrices appearing in equation (26) and the load vector are divided into blocks $\tilde{\mathbf{F}}_{\mathrm{v}}(t)$.

The relative displacements of the contact bonds are $V_j(t) - W_j(t)$, which can be written together as a formula $\mathbf{V}_{\mathrm{c}} - \mathbf{W}_{\mathrm{c}}$, where $\mathbf{W}_{\mathrm{c}} = [W_1, W_2, ..., W_N]^{\mathrm{T}}$, where it is easy to notice that $W_j(t) = w(s_j(t), t)$. In the case of perfectly elastic Hertz springs (see (22), the vectors of the

right-hand sides of equations (25) and (26) have the following general form after performing the calculations

$$\tilde{\mathbf{F}}_{\mathrm{t}} = \tilde{\mathbf{F}}_{\mathrm{Q}} + \tilde{\mathbf{K}}_{\mathrm{tc}}\mathbf{V}_{\mathrm{c}} - \tilde{\mathbf{K}}_{\mathrm{tt}}\mathbf{q}_{\mathrm{t}} \tag{27}$$

$$\tilde{\mathbf{F}}_{\mathrm{v}} = \begin{bmatrix} \varnothing \\ \tilde{\mathbf{K}}_{\mathrm{ct}}\mathbf{q}_{\mathrm{t}} - \{k_{\mathrm{H}}\}\mathbf{V}_{\mathrm{c}} \end{bmatrix} \tag{28}$$

which reveals the coupling of train and track vibrations.

After substituting (27) and (28) to equations (25) and (26), respectively, and taking into account the change in the order of these equations and the internal structure of the $\mathbf{q}_{\mathrm{v}}$ vector, the final matrix equation with a block structure is obtained, which describes the vibrations of the train-track system

$$\begin{bmatrix} \mathbf{B}_{\mathrm{rr}} & \mathbf{B}_{\mathrm{rc}} & \varnothing \\ \mathbf{B}_{\mathrm{cr}} & \mathbf{B}_{\mathrm{cc}} & \varnothing \\ \varnothing & \varnothing & \mathbf{B}_{\mathrm{tt}} \end{bmatrix}\begin{bmatrix} \ddot{\mathbf{r}} \\ \ddot{\mathbf{V}}_{\mathrm{c}} \\ \ddot{\mathbf{q}}_{\mathrm{t}} \end{bmatrix} + \begin{bmatrix} \mathbf{C}_{\mathrm{rr}} & \mathbf{C}_{\mathrm{rc}} & \varnothing \\ \mathbf{C}_{\mathrm{cr}} & \mathbf{C}_{\mathrm{cc}} & \varnothing \\ \varnothing & \varnothing & \mathbf{C}_{\mathrm{tt}} \end{bmatrix}\begin{bmatrix} \dot{\mathbf{r}} \\ \dot{\mathbf{V}}_{\mathrm{c}} \\ \dot{\mathbf{q}}_{\mathrm{t}} \end{bmatrix} + \begin{bmatrix} \mathbf{K}_{\mathrm{rr}} & \mathbf{K}_{\mathrm{rc}} & \varnothing \\ \mathbf{K}_{\mathrm{cr}} & \mathbf{K}_{\mathrm{cc}} + \{k_{\mathrm{H}}\} & -\tilde{\mathbf{K}}_{\mathrm{ct}} \\ \varnothing & -\tilde{\mathbf{K}}_{\mathrm{tc}} & \mathbf{K}_{\mathrm{tt}} + \tilde{\mathbf{K}}_{\mathrm{tt}} \end{bmatrix}\begin{bmatrix} \mathbf{r} \\ \mathbf{V}_{\mathrm{c}} \\ \mathbf{q}_{\mathrm{t}} \end{bmatrix} = \begin{bmatrix} \varnothing \\ \varnothing \\ \tilde{\mathbf{F}}_{\mathrm{Q}} \end{bmatrix} \tag{29}$$

In the case when the contact model is a linearized Hertz-type bond with hysteresis suppression, described by formulas (15) and (23), to determine the generalized load vectors $\tilde{\mathbf{F}}_{\mathrm{t}}$ and $\tilde{\mathbf{F}}_{\mathrm{v}}$ it is necessary to calculate the speed of the track displacement which tracks the position of the *j*th wheel set as it changes with time. According to the idea of the finite element method, the tracking displacement is written by a formula

$$W_j(t) = w(s_j, t) = \sum_{e=1}^{n} \mathbf{N}_e^{\mathrm{T}}(\xi_j)\mathbf{W}_e(t) \tag{30}$$

where $\mathbf{W}_e$ is a vector of boundary displacements of a finite element *e* of length *l*, $\mathbf{N}_e$ is a shape function vector, $\xi_j = (s_j - l(e-1))/l$. The shape functions $\mathbf{N}_e$ are only nonzero within the element *e*, moreover $\xi_j = \xi_j(t)$ because $s_j = vt - d_j$. It follows that

$$\dot{W}_j(t) = \dot{w}(s_j, t) = \sum_{e=1}^{n} \frac{v}{l}\mathbf{N}_e'^{\mathrm{T}}(\xi_j)\mathbf{W}_e(t) + \sum_{e=1}^{n} \mathbf{N}_e^{\mathrm{T}}(\xi_j)\dot{\mathbf{W}}_e(t) \tag{31}$$

where $(\cdot)' = d/d\xi$. After making detailed calculations, it is obtained

$$\tilde{\mathbf{F}}_{\mathrm{t}} = \tilde{\mathbf{F}}_{\mathrm{Q}} + \tilde{\mathbf{K}}_{\mathrm{tc}}\mathbf{V}_{\mathrm{c}} - (\tilde{\mathbf{K}}_{\mathrm{tt}} + \tilde{\mathbf{K}}_{\mathrm{tt}}^{c_{\mathrm{H}}})\mathbf{q}_{\mathrm{t}} + \tilde{\mathbf{C}}_{\mathrm{tc}}\dot{\mathbf{V}}_{\mathrm{c}} - \tilde{\mathbf{C}}_{\mathrm{tt}}\dot{\mathbf{q}}_{\mathrm{t}} \tag{32}$$

$$\tilde{\mathbf{F}}_{\mathrm{v}} = \begin{bmatrix} \varnothing \\ \tilde{\mathbf{K}}_{\mathrm{ct}}\mathbf{q}_{\mathrm{t}} - \{k_{\mathrm{H}}\}\mathbf{V}_{\mathrm{c}} \end{bmatrix} + \begin{bmatrix} \varnothing \\ -\{d_{\mathrm{H}}\}\dot{\mathbf{V}}_{\mathrm{c}} + \tilde{\mathbf{K}}_{\mathrm{ct}}^{c_{\mathrm{H}}}\mathbf{q}_{\mathrm{t}} + \tilde{\mathbf{C}}_{\mathrm{ct}}\dot{\mathbf{q}}_{\mathrm{t}} \end{bmatrix} \tag{33}$$

which leads to a system of motion equations

$$\begin{bmatrix} \mathbf{B}_{\mathrm{rr}} & \mathbf{B}_{\mathrm{rc}} & \varnothing \\ \mathbf{B}_{\mathrm{cr}} & \mathbf{B}_{\mathrm{cc}} & \varnothing \\ \varnothing & \varnothing & \mathbf{B}_{\mathrm{tt}} \end{bmatrix}\begin{bmatrix} \ddot{\mathbf{r}} \\ \ddot{\mathbf{V}}_{\mathrm{c}} \\ \ddot{\mathbf{q}}_{\mathrm{t}} \end{bmatrix} + \begin{bmatrix} \mathbf{C}_{\mathrm{rr}} & \mathbf{C}_{\mathrm{rc}} & \varnothing \\ \mathbf{C}_{\mathrm{cr}} & \mathbf{C}_{\mathrm{cc}} + \{D_{\mathrm{H}}\} & -\tilde{\mathbf{C}}_{\mathrm{ct}} \\ \varnothing & -\tilde{\mathbf{C}}_{\mathrm{tc}} & \mathbf{C}_{\mathrm{tt}} + \tilde{\mathbf{C}}_{\mathrm{tt}} \end{bmatrix}\begin{bmatrix} \dot{\mathbf{r}} \\ \dot{\mathbf{V}}_{\mathrm{c}} \\ \dot{\mathbf{q}}_{\mathrm{t}} \end{bmatrix} +$$
$$\begin{bmatrix} \mathbf{K}_{\mathrm{rr}} & \mathbf{K}_{\mathrm{rc}} & \varnothing \\ \mathbf{K}_{\mathrm{cr}} & \mathbf{K}_{\mathrm{cc}} + \{k_{\mathrm{H}}\} & -\tilde{\mathbf{K}}_{\mathrm{ct}} - \tilde{\mathbf{K}}_{\mathrm{ct}}^{c_{\mathrm{H}}} \\ \varnothing & -\tilde{\mathbf{K}}_{\mathrm{tc}} & \mathbf{K}_{\mathrm{tt}} + \tilde{\mathbf{K}}_{\mathrm{tt}} + \tilde{\mathbf{K}}_{\mathrm{tt}}^{c_{\mathrm{H}}} \end{bmatrix}\begin{bmatrix} \mathbf{r} \\ \mathbf{V}_{\mathrm{c}} \\ \mathbf{q}_{\mathrm{t}} \end{bmatrix} = \begin{bmatrix} \varnothing \\ \varnothing \\ \tilde{\mathbf{F}}_{\mathrm{Q}} \end{bmatrix} \tag{34}$$

In both considered cases of contact springs, the solution of the equations of motion is obtained using the classical recursive numerical integration scheme, e.g. one of the β-Nemark methods

Train-track vibration simulations

Based on the obtained equations of motion (29) and (34), an original program of vibration simulation in the Python 3 computing environment was developed. Integration of the equations over time was performed using the Newmark-Wilson method with the parameter $\beta = 1/4$, the time step was $\Delta t = 0,0001\,\mathrm{s}$. Finite elements with a length of 0.5 m were used for track discretization. A train consisting of three carriages runs along a 100-meter long track section, in the middle of which there is a threshold unevenness resulting from a step-change in the surface stiffness of the track substrate: from $5 \cdot 10^7\,\mathrm{kN/m^3}$ to $25 \cdot 10^7\,\mathrm{kN/m^3}$. Elasticity coefficients of the base of the track modeling beam were calculated assuming the width of the support equal to the length of the rail sleeper 2.6 m. Other parameters adopted for calculations are presented in Table **1**, while the data for the vehicle was taken from the monograph by Klasztorny [5].

Tab. 1. Input parameters

Parameter	Value
Travel speed	$60\,\mathrm{m/s}$
Retardation time (related to rail material)	$2,1 \cdot 10^{-5}\,\mathrm{s}$
Rail	60E1
Substrate modulus of elasticity 1	$1,3 \cdot 10^8\,\mathrm{N/m^2}$
Substrate modulus of elasticity 2	$7,5 \cdot 10^8\,\mathrm{N/m^2}$
Ground suppression	$2,8667 \cdot 10^5\,\mathrm{Ns/m}$
Body weight	$36000\,\mathrm{kg}$
Trolley weight	$4950\,\mathrm{kg}$
Wheelset weight	$2400\,\mathrm{kg}$
Moment of rotational inertia of the body mass	$1894000\,\mathrm{kgm^2}$
Moment of inertia of the rotational mass of the trolley	$6150\,\mathrm{kgm^2}$
Half the distance between the axles of the bogies	$8,75\,\mathrm{m}$
Half the distance between the wheelsets on the carriage	$1,25\,\mathrm{m}$
Lower vehicle suspension damping	$2 \cdot 9815\,\mathrm{Ns/m}$
Upper vehicle suspension damping	$2 \cdot 21675\,\mathrm{Ns/m}$
The rigidity of the lower suspension of the vehicle	$2 \cdot 1270000\,\mathrm{N/m}$
The stiffness of the upper suspension of the vehicle	$2 \cdot 443500\,\mathrm{N/m}$
Vehicle wheel radius	$0,46\,\mathrm{m}$
The radius of the rail at the point of contact	$0,3\,\mathrm{m}$

The aim of the numerical analysis was to compare the simulation results of the train-track system vibrations obtained with the use of two different models of the contact bond at the wheel-rail interface. The vehicle and hence the railway track vibrate when the vehicle enters a deformable track section from a non-deformable track, and then travels through the threshold unevenness of the track at a speed of 60 m/s (216 km/h). The simulation results shown in Figures **3-7** are fragments of time courses of selected train-track system responses, which illustrate the dynamic effect caused by the threshold unevenness of the track.

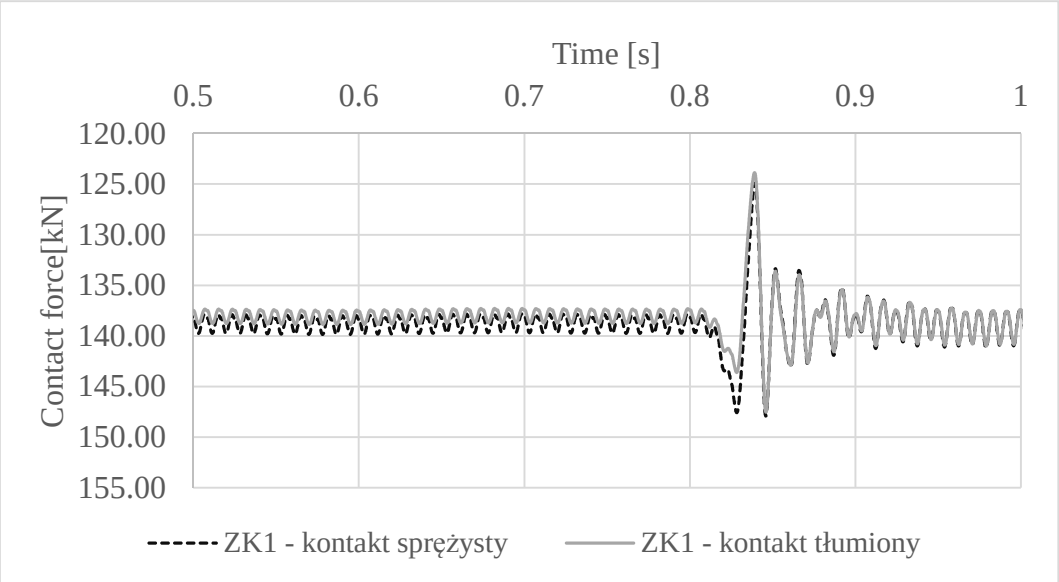

3. Force in the contact bond of wheelset No.1

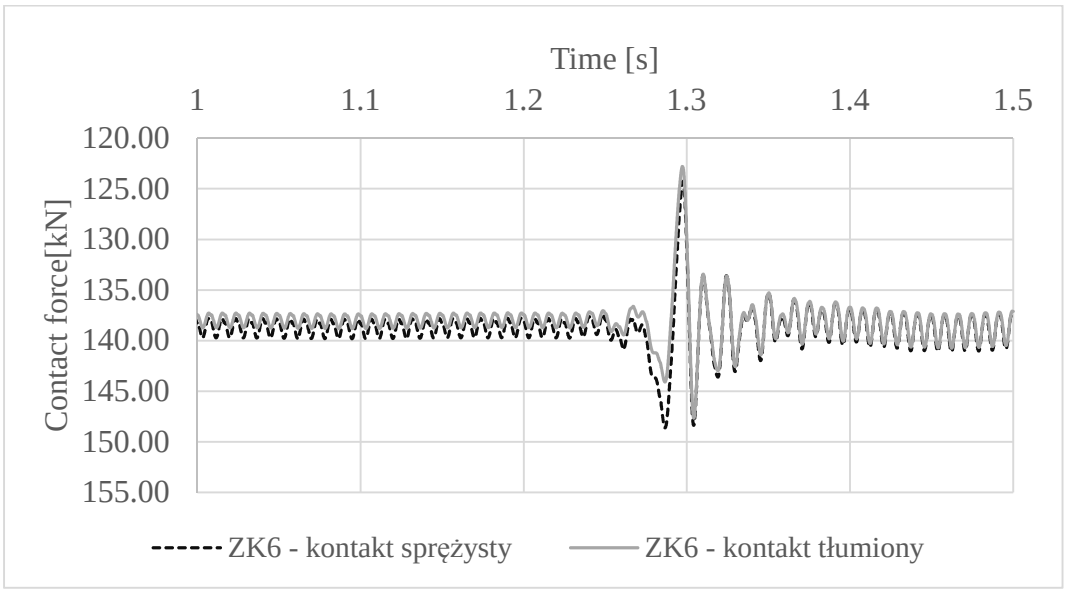

4. Force in the contact bond of wheelset No. 6

Figure **3** shows two graphs of changes in the contact force with time between the first wheelset and the track. The corresponding results for the sixth wheelset are shown in Figure **4**. In both cases, the contact force oscillates around the static pressure force of 138.5 kN. The dynamic threshold effect is manifested here by three large peaks, then the contact force oscillations decrease. As a measure of the threshold effect, the value of the contact force peak related to static pressure and expressed as a percentage can be taken. Then, in the case of an elastic contact bond and the first wheelset, successive peaks are: 106%, 90%, and 107%, and in the case of an elastic-damping bond: 104%, 89%, and 106.5%. Similar results are obtained for the sixth wheelset. It follows that the use of an elastic-damping contact bond instead of the classic perfectly elastic bond, which is tantamount to taking into account the damping in the wheel-rail contact zone, reduces the incremental peaks (first and third) of the contact force, occurring after the wheelset has passed through the threshold unevenness. This effect is

clearly visible in the case of the first strength peak, while it is poorly manifested in the next ones.

It is worth noting that both the first and the third peaks are an increase in the contact force, unfavorable due to the condition of the track strain (incremental peaks). From this point of view, simplifying the contact model to a perfectly elastic bond is a conservative solution as it gives overestimated results. The opposite is true for the second peak, which corresponds to a reduction in the contact force and thus the track contact force. It can be assumed that with the increase of the driving speed, the peak value will increase, which in an extreme situation may lead to the loss of wheel-rail contact. In this aspect, the use of a simplified contact model is not advantageous as it underestimates the threshold effect.

The next three figures show fragments of the generated vibration waveforms and the acceleration of the track vibrations just after the threshold unevenness (Figures **5** and **6**) and the vibration accelerations of the first wheelset (Figure **7**). As can be seen from the presented graphs, the impact of damping in the contact zone is practically invisible at the assumed train speed (60 m / s). It should be emphasized that the track vibration results shown from the point of view of a stationary observer, i.e. in a specific track section, do not allow for the analysis of the threshold effect (Figures **5** and **6**). They should be compared with simulations of a train running through a track devoid of threshold unevenness and calculations should be made for at least several consecutive sections. This is an ineffective approach. A better alternative would be to observe the vibrations from the position of a moving observer, i.e. the analysis of vibrations in the contact cross-section of the track. Such a "tracking" answer is, inherently, the course of the vibrations of the wheelset (Figure **7**). It is worth noting that also, in this case, the application of the elastic-damping bond does not have a noticeable effect on the simulation results.

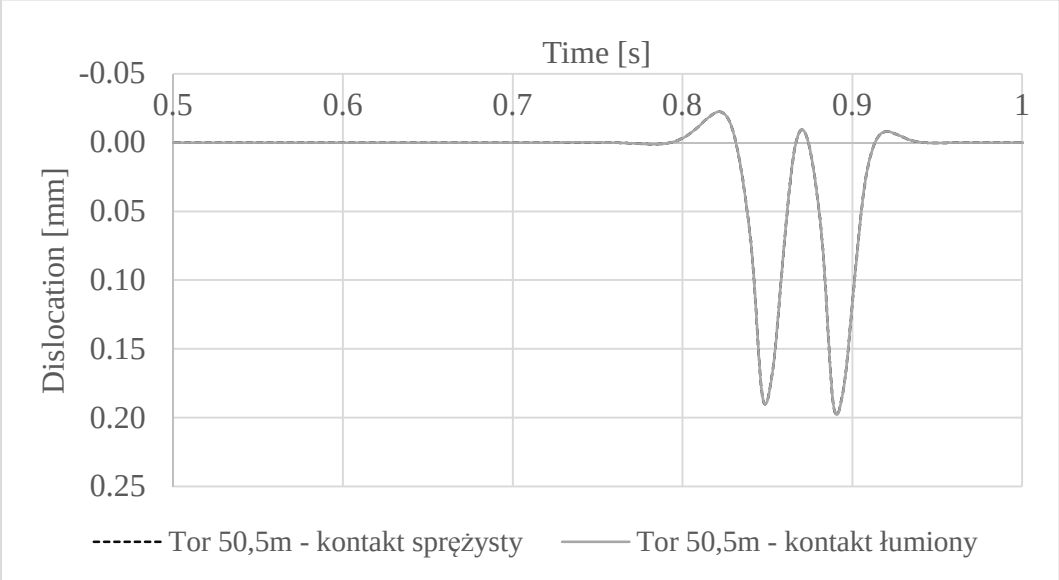

5. The track movement in section directly behind the threshold unevenness

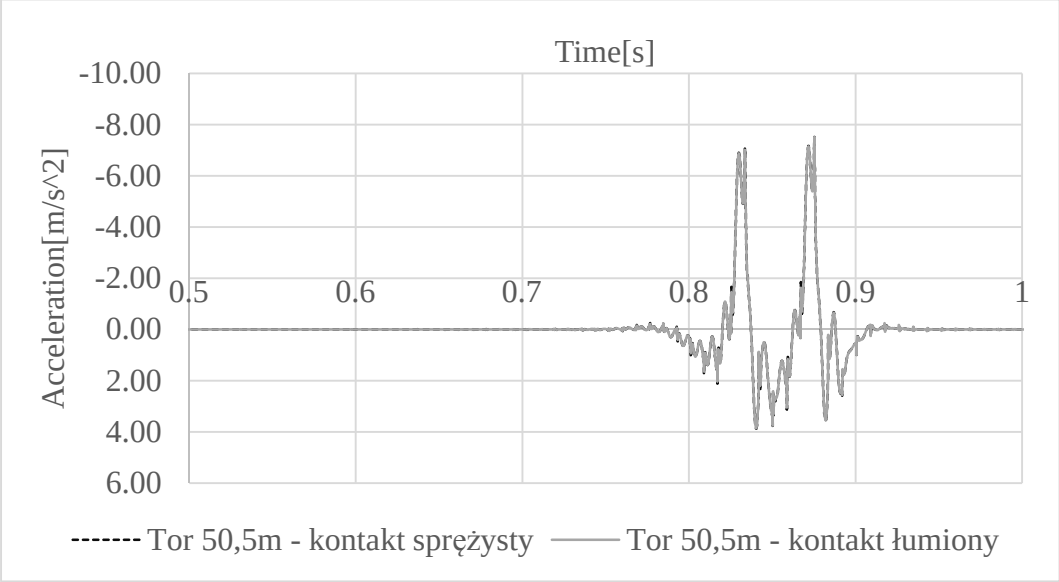

6. Acceleration of track vibrations in the cross-section located directly behind the threshold unevenness

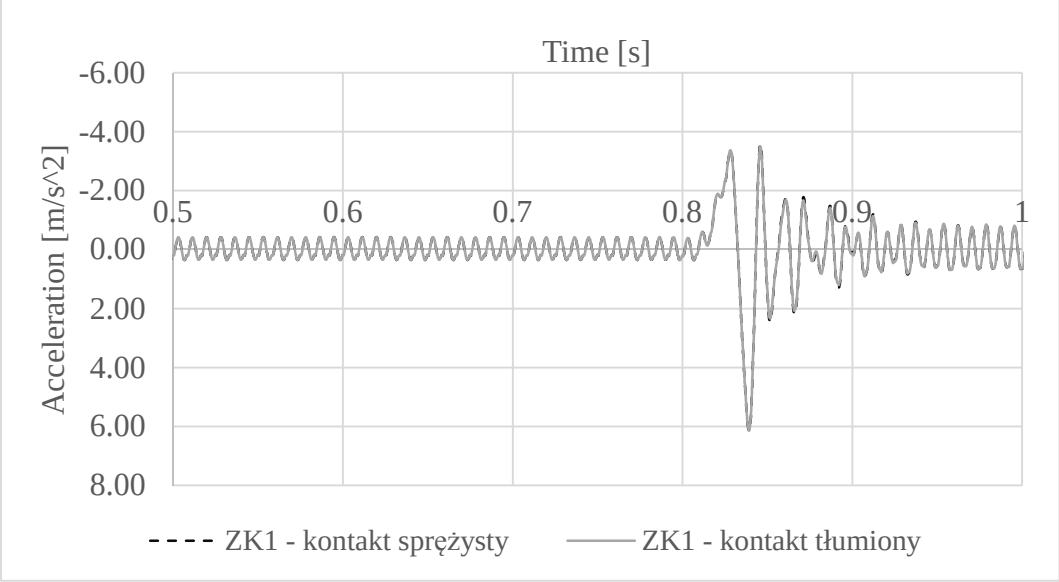

7. Vibration acceleration of wheelset No. 1

Figure **7** shows a clearly visible threshold effect in the vibration acceleration of the wheelset. The greatest acceleration peak is associated with the largest (second) peak in the contact force (Figure **3**). The vertical movement of the wheelset with positive acceleration results in the opposite inertia force, which reduces the static track force in the case under consideration to approx. 90%. It should be emphasized that this observation confirms the proper functioning of the developed algorithm and software - in line with intuition and experience.

General conclusions

Based on the performed numerical analyzes, it can be concluded that the use of the wheel-rail contact model enriched with hysteresis suppression makes sense when the tests are focused on the track strain, and going further - on the fatigue effects in the track and railway vehicle. This is due to the fact that the damping on the wheel-rail contact significantly influences the contact force, which is also the force that loads the track and the vehicle. In the analysis of the stress state and fatigue analyzes, if they are to refer to high-speed railways, it is advisable to simultaneously take into account the one-sided operation of the contact bonds in order to describe the situations of loss of contact observed in operational practice. t has been shown that omitting the damping in the contact zone disturbs the correct identification of the contact loss phenomenon. It lowers the probability of a loss of contact because the track relief is then underestimated (the peak of contact force decreases, which reduces the static pressure). The above conclusions should be treated as preliminary. To confirm them, a much more extensive numerical analysis is needed, including studies of the impact of operational speeds, including the analysis of the track effort state based on a modified algorithm taking into account one-sided contact springs.

Source materials

[1] Bosso N., Spiryagin M., Gugliotta A., Somá A., *Mechatronic modeling of real-time wheel-rail contact*, Springer-Verlag, Berlin Heidelberg, 2013.
[2] Bryja D., Chojnacki W., *Dwustronna więź kontaktowa Hertz'a w numerycznej analizie drgań sprzężonego układu pociąg-tor*, Przegląd Komunikacyjny, 2019, r. 74, nr 11, 2-7.
[3] Esveld C., *Modern railway track*, MRT-Productions, The Netherlands, 2014.
[4] Johnson K. L., *Contact mechanics*, Cambridge University Press, Cambridge, 1985.
[5] Klasztorny M., *Dynamika mostów belkowych obciążonych pociągami szybkobieżnymi*, Wydawnictwa Naukowo-Techniczne, Warszawa, 2005.
[6] Knothe K., Stichel S., *Rail vehicle dynamics*, Springer, Cham, 2017.
[7] Lankarani H., Nikravesh P., *A contact force model with hysteresis damping for impact analysis of multibody systems*, Journal of Mechanical Design, 1990, vol 112, 369-376.
[8] Lee T., Wang A., *On the dynamics of intermittent – motion mechanisms, Part I. Dynamic model and response*, Journal of Mechanisms Transmissions and Automation in Design – Transactions of the ASME, 1983, vol 105, 534-540.
[9] Podwórna M., Klasztorny M., *Wpływ cech pojazdów szynowych na odpowiedź dynamiczną mostu belkowego*, Drogi i Mosty, 2011, nr. 3, 63-87.
[10] Pombo J., Ambrosio J., Silva M., *A new wheel – rail contact model for railway dynamics*, Vehicle System Dynamics, 2007, vol 45, 165-189.
[11] Shabana A., Zaazaa K. Escalona J. Sany J. *Development of elastic force model for wheel/rail contact problems*, Journal of Sound and Vibration, 2004, vol 269, 295-325.
[12] Skrinjar L., Slavic J., Boltezar M., *A review of continuous contact – force models in multibody dynamics*, International Journal of Mechanical Science, 2018, vol 145, 171-187.
[13] Sun Y.Q., Dhanasekar M., *A dynamic model for the vertical interaction of the rail track and wagon system*, International Journal of Solids and Structures, 2002, vol 39, s. 1337-1359.
[14] Xu L., Zhai W., *A three-dimensional model for train-track-bridge dynamic interactions with hypothesis of wheel-rail rigid contact*, Mechanical Systems and Signal Processing, 2019, vol. 132, 471-489.
[15] Xu X. Y., Li Y. L., *Dynamic analysis of wind-vehicle-bridge system based on rigid-flexible coupling method*, Advances in Civil, Environmental, and Materials Research ACEM16, 28.08.2016.

[16] Zhai W., Sun X., *A detailed model for investigating vertical interaction between railway vehicle and track*, International Journal of Vehicle Mechanics and Mobility, 1994, vol. 23, 603-615
[17] Zhai W., *Two simple fast integration methods for large – scale dynamic problems in engineering*, International Journal for Numerical Methods in Engineering, 1996, vol. 39, 4199-4214
[18] Zhai W., *Vehicle – Track coupled dynamics theory and applications*, Springer, Science Press Beijing, 2020